Altered volcanic deposits as basal failure surfaces of submarine landslides

Elda Miramontes*, Nabil Sultan, Sébastien Garziglia, Gwenael Jouet, Ewan Pelleter, and Antonio Cattaneo
IFREMER, Géosciences Marines, 29280 Plouzané, France

ABSTRACT

One of the main concerns regarding the development of submarine landslides is the role played by weak layers in the failure process and, in particular, their impact in terms of volume, shape and evolution of mass movements. In the present study we identified a weak layer in the eastern margin of the Corsica Trough (northern Tyrrhenian Sea) that formed the basal failure surface of the Pianosa Slump at 42–50 ka. This layer is characterized by high water content, high plasticity, high compressibility, and post-peak strain softening behavior (i.e., strength loss with increasing strain). These specific mechanical and sedimentological properties seem to be related to the presence of analcime zeolites with a concentration of 2–4% in the muddy sediment. Zeolites commonly form by the alteration of volcanic rocks and were deposited on the slope during a sea level low-stand. The influence of the zeolitic layer on slope instability was tested numerically using an elastic-perfectly plastic model that exhibits strain softening. Modeling results show that erosion at the foot of the slope could lead to enough strain to reduce the shear strength of the zeolitic layer and lead to slip in this layer. We conclude that the strain softening behavior of muddy zeolitic sediment plays an important role in predisposing submarine landslides on continental slopes.

INTRODUCTION

The large size of submarine landslides compared to their terrestrial counterparts is related, among other factors, to the presence of extended weak layers within marine sediments accumulated along continental slopes (Puzrin et al., 2016). Locat et al. (2014) pointed out that weak layers may be inherited from the original properties of sediment or induced by external factors. Strain softening behavior is widely considered as a major factor in the development of large-scale progressive failure, as demonstrated for the Storegga slide (Dey et al., 2016). Understanding the mechanical and sedimentological properties of weak layers is the key to identifying the potential failure surface of submarine landslides and to modeling their lateral propagation (Puzrin et al., 2016). In this work, we suggest that zeolites, a product of volcanic rock alteration (Mumpton, 1999), influence the sedimentological and geotechnical properties of fine marine sediment and contribute to the development of slope failure. This finding has potentially broad impact since many regions in the world contain abundant volcanic material that can be a potential source of zeolites (Fig. 1).

A ZEOLITIC WEAK LAYER

The Pliocene-Quaternary sedimentary deposits along the Pianosa Ridge (northern Tyrrhenian Sea) are composed of muddy contourites that were affected by multiple mass-wasting events (Fig. 2A; Miramontes et al., 2016, 2018). The most recent of them, called the Pianosa Slump (PS), occurred between 42 and 50 ka in a convex-shaped contourite, flanked by zones of focused erosion (moats) at the foot of the slope, where slopes reach 10–16° (Fig. 2A; Miramontes et al., 2018). The timing of the Pianosa Slump formation coincides with a period of sea-level fall (between 52 and 48 k.y. B.P.), during which erosion at the moats was enhanced due to an increase in bottom-current intensity (Miramontes et al., 2016).

The PS headwall is located at 500–670 m water depth and the scar is currently covered by 20 m of sediment (Figs. 2B and 2C). Multi-channel high resolution mini GI gun (50–250 Hz) and sub-bottom profiler (SBP; 1800–5300 Hz) seismic reflection data, acquired during the PRISME2 cruise in 2013 (R/V *L'Atalante*; https://doi.org/10.17600/13010050), show that the basal failure surface of the PS follows a regional stratigraphic horizon marked on seismic profiles by high-amplitude reflections (Figs. 2B and 2C). At the time of failure, this horizon was at ~35 m below the seafloor (mbsf; Figs. 2B and 2C), and its age has been estimated at ca. 150 ka based on the chronology proposed by Miramontes et al. (2016). In three Calypso piston cores (CS11, CS12 and CS21), collected in undisturbed areas during the PRISME3 cruise in 2013 (R/V *Pourquoi pas?*; https://doi.org/10.17600/13030060) (Fig. 2A), this horizon

corresponds to a 2–4-m-thick layer. X-ray diffraction analyses on 12 samples from cores CS12, CS17, and CS21 revealed that, in contrast to the adjacent sediment, this particular layer contains analcime zeolitic minerals in a mass concentration of 2–4 wt% (Table DR1 in the GSA Data Repository[1]). This difference in bulk mineralogy is not associated with a significantly different clay mineralogical composition (Table DR2) or grain size (Fig. DR3). The scanning electron microscope (SEM) image of a zeolitic sediment thin section shows that zeolites are uniformly distributed in the sediment and have a typical diameter of ~50–100 μm (Fig. 3A). Although deeply buried, this particular sediment has a water content as high as 89 wt%, similar to that of surface sediment values (Fig. 3B). The sediment water content (related to sediment porosity) and zeolite content tend to be linearly correlated (Table DR4, Fig. DR5). The liquid limits obtained by the fall cone method are very high (up to 100%) for zeolitic sediments compared to non-zeolitic sediments that are always below 77% (Fig. DR6). Therefore, despite its high water content, the zeolitic sediment is not in a state of potential flow. Plasticity indices are also high for the zeolitic sediment (50–70), twice the values obtained from the adjacent sediment (Fig. 3B). Based on oedometer test data, all the sediments are normally consolidated, but those containing zeolites exhibit a higher (post-gross yield) compressibility (Fig. DR7).

In order to determine the strength properties of the sediments, we performed seven consolidated anisotropic undrained compression (CAUC) triaxial tests on samples from cores CS12 and CS21 (Table DR8, Fig. DR9). These tests revealed that the undrained shear strength of the zeolitic sediment reaches a peak value at lower strains than the adjacent sediment: at 2% of axial strain, in contrast to 8% for the non-zeolitic sediment. Moreover, the zeolitic sediment displays a more pronounced strain softening; its

*Current address: CNRS, UMR6538, Laboratoire Géosciences Océan, IUEM-UBO, 29280 Plouzané, France; E-mail: Elda.Miramontesgarcia@univ-brest.fr
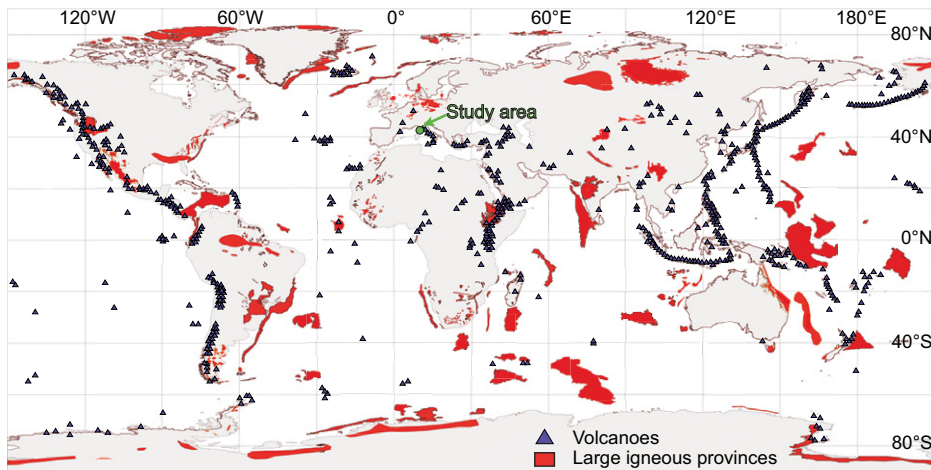
Figure 1. World distribution of large igneous provinces (modified from Bryan and Ferrari, 2013) and volcanoes (Venzke, E., 2013), as potential sources of zeolites.
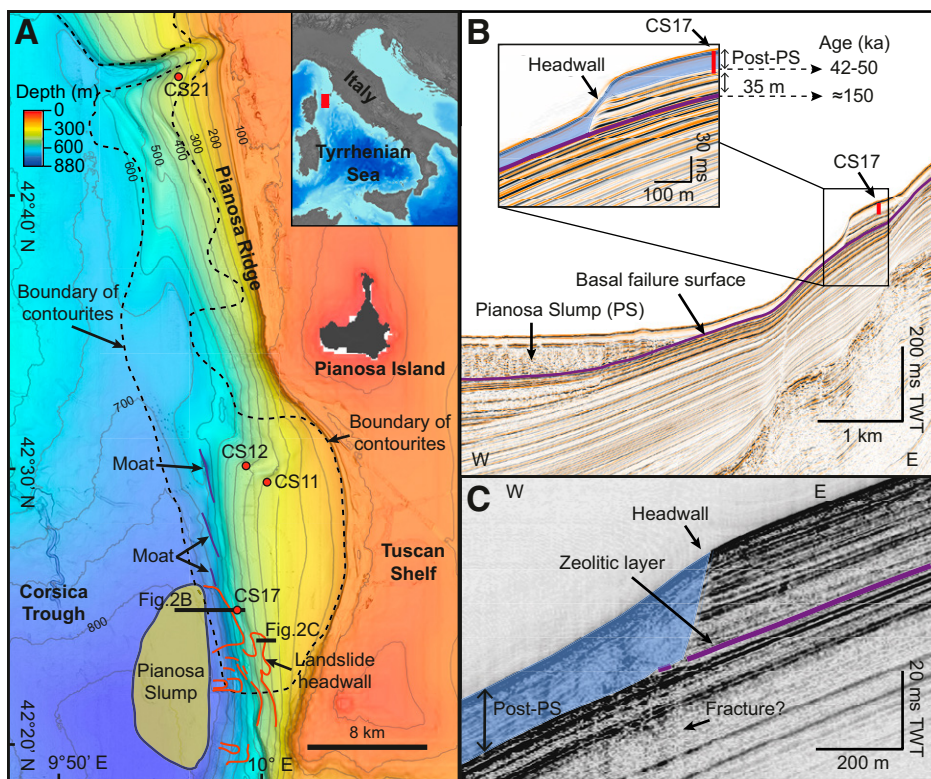

Figure 2. A: Multibeam bathymetry of the Pianosa Ridge, with location of sediment cores (red dots), contourites (dashed black line), moats (blue lines), the Pianosa Slump deposit (yellow), and the landslide headwall (red lines) .The bathymetric contour interval is 50 m, starting at 50 m water depth. B: Seismic profile PSM2-HR-033 multichannel high-resolution mini GI gun seismic reflection profile showing the Pianosa Slump deposit, the headwall, and the basal failure surface. TWT—two-way time. C: PSM2-CH-061 sub-bottom profiler line located at the headwall of the Pianosa Slump, showing location of the zeolitic layer.

undrained shear strength is reduced by 33% at 15% strain (Fig. 4).

SLOPE STABILITY MODELING

The influence of the strain-softening zeolitic layer on slope instability is simulated with the commercial software Plaxis 2D (https://www .plaxis.com/product/plaxis-2d/, Brinkgreve et al., 2012). The model geometry is divided into 12 sedimentary layers, 5 m thick, except for the zeolitic layer that is 3 m thick (at 35–38 mbsf) and the deepest layer that is 7 m thick (at 53–60 mbsf) (Fig. 5A; Table DR10). The initial slope angle in the zone of the moat is 10.5° (Fig. 5A). The sediment layers are modeled as a Mohr-Coulomb material. The zeolitic layer is also modeled as an elastic–perfectly plastic material, but an approximated strain-softening approach is used to simulate the post-peak shear strength loss by applying the method proposed by Lobbestael et al. (2013), based on Lo and Lee (1973) and Potts et al. (1990). The approach consists of tracking the plastic strains and reducing the shear strength accordingly, using the stress-strain curve obtained from the CAUC triaxial test carried out on a zeolitic sediment sample (Fig. 4). The zeolitic layer is laterally divided into small sections (50 m long and 3 m high) to locally reduce the strength parameters in successive steps. In order to reproduce the observed slope geometry, we simulated a total erosion of 5 m at the moat by removing 1 m of sediment in five successive steps. The erosion is maximal at the central part of the moat, decreasing to zero over a distance of 200 m upslope and downslope of the central part of the moat (Fig. 5A). We performed the slope stability calculation under undrained conditions because the development of catastrophic failure, which is the most critical scenario, is expected to occur very rapidly and will thus mobilize the undrained parameters of the sediment (Puzrin et al., 2016).

The slope stability analysis performed before the erosion phases provides a factor of safety (FOS) of 1.15 with a shallow potential failure surface (Fig. 5A). After the first erosion phase and the induced strain softening within the zeolitic layer, the failure surface is deeper, crossing the particular layer (Fig. 5B). Increasing erosion at the foot of the slope induces a lengthening of the shear zone within the zeolitic layer (Figs. DR12 and DR13). According to the numerical model results, a 5 m erosion would trigger the collapse of the slope (i.e., FOS < 1).

DISCUSSION AND CONCLUSION

Role of Zeolites in Slope Stability

The basal shear zone of the Pianosa Slump formed in a zeolitic layer (with high water content, plasticity, and compressibility) that tends to readily soften when sheared undrained. The compressibility of clays depends not only on their mechanical properties, but also on the soil physico-chemical properties (Bolt, 1956). The diffuse double layer (DDL) theory of Gouy-Chapman explains the ionic distribution around clay minerals, which generally are negatively charged (Bolt, 1956). According to this theory, the DDL thickens with a reduction in the ionic concentration and/or in the ionic valence, resulting in an increase of the sediment porosity (Bolt, 1956). Zeolites are widely used in agriculture and industry applications due to their high cation exchange capacities, that can be higher than in clays (Mumpton, 1999). Zeolite particles in marine fine-grained sediment could attract more cations than the clay particles, resulting
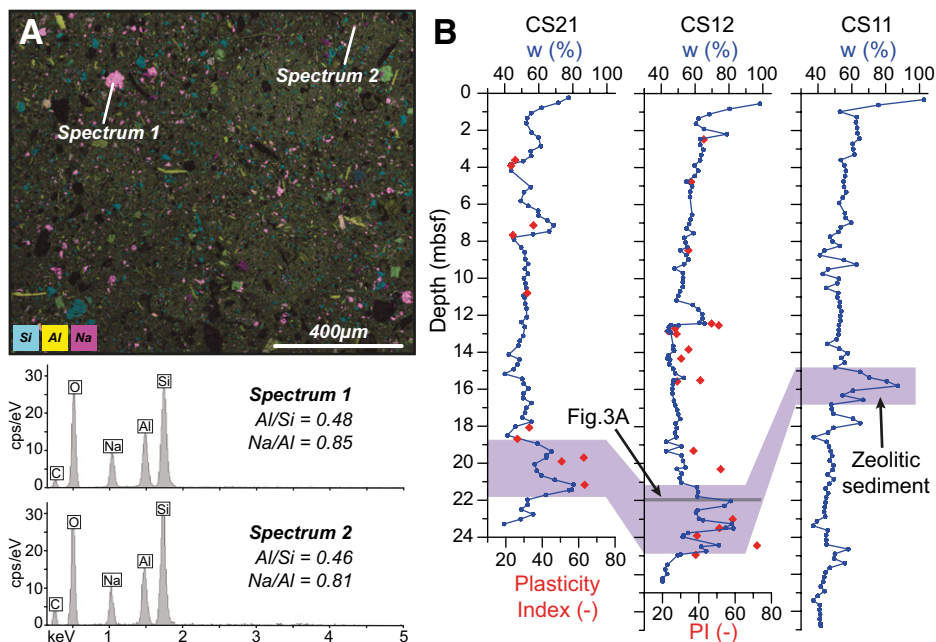
Figure 3. A: Chemical composition map, obtained with a scanning electron microscope, of a zeolitic sediment thin section (core CS12, at 21.9–22.0 m) showing the zeolites in pink, and typical spectra of zeolites. Note that zeolites are uniformly distributed in the sediment, with a typical diameter of ~50–100 μm. cps/eV—counts per second per electron volt. B: Water content (w) of the three sediment cores that sampled the zeolitic sediment layer, and plasticity index (PI) of cores CS21 and CS12.
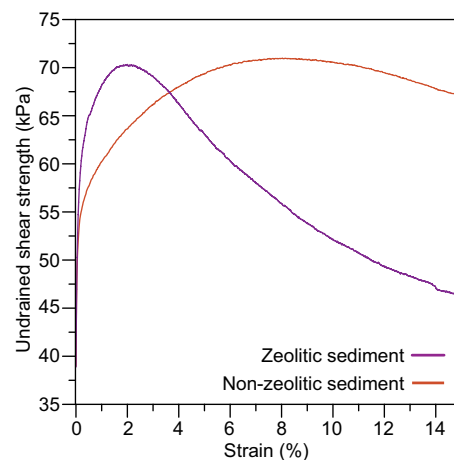

Figure 4. Undrained shear strength obtained from consolidated anisotropic undrained compression (CAUC) triaxial tests performed on one zeolitic sediment sample from core CS21 (purple line, at 21.31–21.47 mbsf) and one non-zeolitic sediment sample from core CS12 (red line, at 26.28–26.42 mbsf). The mean effective stress after saturation and consolidation applied in each test was 127 kPa.

in a decrease of the cation concentration in the vicinity of clays. Consequently, according to the Gouy-Chapman theory and Bolt (1956), the DDL of clay particles and the repulsive forces would increase, generating a weak sediment structure with higher porosity and compressibility (Fig. DR11). Because zeolites are uniformly distributed in the failed sediment layer (Fig. 3A), this process could affect the whole zeolitic layer.

The results of the slope stability analysis show that erosion in the moat, located at the foot of the slope, can generate enough strain to substantially reduce the strength of the zeolitic layer due to its strain-softening behavior (Fig. 5).

Simulations also show that successive erosion phases generate a progressive lengthening of the initial softened zone (Fig. DR12). The predicted failure surface appears to develop along the softened zone but does not extend upslope as much as is observed for the PS (Fig. 5). This is attributable to model limitations in simulating stress transmission from a softened zone to the neighboring undisturbed sediment, as is expected to occur under existing or additional external forces in catastrophic or progressive failure, respectively (Puzrin and Germanovich, 2005).

Our findings concerning the mechanism of weak layer formation in fine-grained marine

sediment with altered volcanic deposits could apply to all continental margins close to zones with volcanic material (Fig. 1). The strength of a zeolitic layer could be reduced by erosion, as in the Pianosa Ridge, but it could be also reduced by other external processes such as seismic loading, overloading and steepening.

Origin and Distribution of Zeolites in Marine Sediments

The origin of zeolites in the Pianosa Ridge is probably not linked to the burial metamorphism of volcanic ashes because it was at only 35 mbsf at the time of the mass failure, and this type of alteration usually happens hundreds of meters below the surface (Wiemer and Kopf, 2015). Moreover, *in situ* formation of zeolites in the marine sediment is unlikely due to the lack of
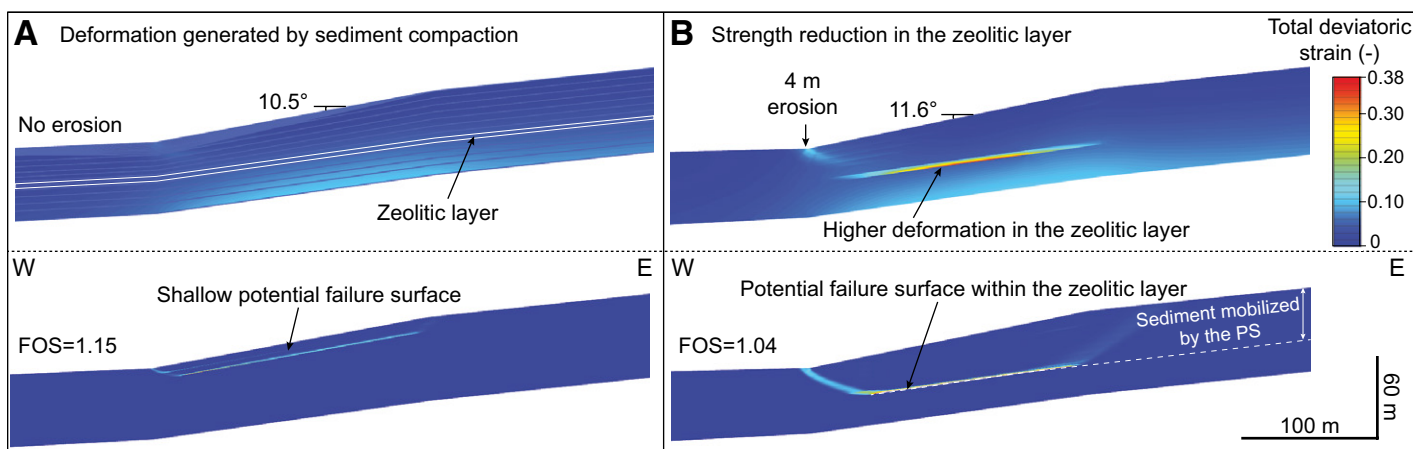

Figure 5. Total deviatoric strain after sediment consolidation (A) and after the strength reduction in the zeolitic layer caused by a 4 m erosion in the moat (B). The lower plots show the critical failure surface at stages A and B. The observed failure surface of the Pianosa Slump (PS) is marked with a dashed white line. FOS—factor of safety.

volcanic ash in the Corsica Trough. Zeolites were probably produced in the Tuscan magmatic province (Dini et al., 2002) and then transported to the continental slope, resulting in an essentially uniform distribution of the zeolites in the sediment (Fig. 3A). For instance, the basalts present on Elba Island (Dini et al., 2002) could have been altered to yield analcime, which is the typical zeolite type formed from basalts (Coombs et al., 1959). At the time of the zeolitic layer deposition (150 ka), the sea level was ~100 m below the present-day level (Rohling et al., 2014) and the shoreline was almost at the shelf edge, favoring the erosion of the zeolites in the Tuscan Shelf, and their accumulation in the eastern flank of the Corsica Trough (Fig. 2A). Previous studies showed that zeolites can be transported and deposited at hundreds of kilometers away from their formation site: zeolites present in hemipelagic sediment of the western North Atlantic were interpreted as being detrital (Houghton et al., 1979), and Zúñiga et al. (2007) identified a fine-grained turbidite rich in zeolites in the Balearic abyssal plain, probably originated on the Sardinian continental margin and also characterized by high water contents.

The presence of zeolites has been widely documented in volcanic settings; for example, in the circum-Pacific arc (Machiels et al., 2014), in the Antilles volcanic arc (Jolly et al., 2001), in the Mediterranean Sea (Altaner et al., 2013), and in volcanic islands such as the Canary Islands (Donoghue et al., 2008), Cape Verde (Barker et al., 2009), Hawaii (Morgan and Clague, 2003), or Reunion (Bachèlery et al., 2003). The formation of sediment layers rich in zeolites can be extended in time and is not only restricted to the period of zeolitic mineral formation, since the minerals can be stocked onshore or on the continental shelf and later transported to the continental slope. Detecting the presence of zeolites in marine sediments may help to understand the preconditioning conditions of submarine landslides on continental margins close to volcanic zones.

REFERENCES CITED
Altaner, S., Demosthenous, C., Pozzuoli, A., and Rolandi, G., 2013, Alteration history of Mount Epomeo Green Tuff and a related polymictic breccia, Ischia Island, Italy: Evidence for debris avalanche: Bulletin of Volcanology, v. 75, p. 718, https://doi.org/10.1007/s00445-013-0718-1.

Bachèlery, P., Robineau, B., Courteaud, M., and Savin, C., 2003, Avalanches de débris sur le flanc occidental du volcan-bouclier Piton des Neiges (Réunion): Bulletin de la Société Géologique de France, v. 174, p. 125–140, https://doi.org/10.2113/174.2.125.

Barker, A.K., Holm, P.M., Peate, D.W., and Baker, J.A., 2009, Geochemical stratigraphy of submarine lavas (3–5 Ma) from the Flamengos Valley, Santiago, southern Cape Verde islands: Journal of Petrology, v. 50, p. 169–193, https://doi.org/10.1093/petrology/egn081.

Bolt, G.H., 1956, Physico-chemical analysis of the compressibility of pure clays: Geotechnique, v. 6, p. 86–93, https://doi.org/10.1680/geot.1956.6.2.86.

Brinkgreve, R.B.J., Engin, E., and Swolfs, W.M., 2012, PLAXIS 2D 2012 Manual: Delft, Netherlands, Delft University of Technology and PLAXIS, 14 p.

Bryan, S.E., and Ferrari, L., 2013, Large igneous provinces and silicic large igneous provinces: Progress in our understanding over the last 25 years: Geological Society of America Bulletin, v. 125, p. 1053–1078, https://doi.org/10.1130/B30820.1.

Coombs, D.S., Ellis, A.J., Fyfe, W.S., and Taylor, A.M., 1959, The zeolite facies, with comments on the interpretation of hydrothermal syntheses: Geochimica et Cosmochimica Acta, v. 17, p. 53–107, https://doi.org/10.1016/0016-7037(59)90079-1.

Dey, R., Hawlader, B., Phillips, R., and Soga, K., 2016, Numerical modeling of submarine landslides with sensitive clay layers: Geotechnique, v. 66, p. 454–468, https://doi.org/10.1680/jgeot.15.P.111.

Dini, A., Innocenti, F., Rocchi, S., Tonarini, S., and Westerman, D.S., 2002, The magmatic evolution of the late Miocene laccolith-pluton-dyke granitic complex of Elba Island, Italy: Geological Magazine, v. 139, p. 257–279, https://doi.org/10.1017/S0016756802006556.

Donoghue, E., Troll, V.R., Harris, C., O'Halloran, A., Walter, T.R., and Perez Torrado, F.J., 2008, Low-temperature hydrothermal alteration of intra-caldera tuffs, Miocene Tejeda caldera, Gran Canaria, Canary Islands: Journal of Volcanology and Geothermal Research, v. 176, p. 551–564, https://doi.org/10.1016/j.jvolgeores.2008.05.002.

Houghton, R.L., Rothe, P., and Galehouse, J.S., 1979, Distribution and chemistry of phillipsite, clinoptilolite, and associated zeolites at DSDP sites 382, 385, and 386 in the western North Atlantic, *in* Tucholke, B.E., et al., eds., Initial Reports of the Deep Sea Drilling Project: Washington, D.C., U.S. Government Printing Office, v. 43, p. 463–483, https://doi.org/10.2973/dsdp.proc.43.115.1979.

Jolly, W.T., Lidiak, E.G., Dickin, A.P., and Wu, T.W., 2001, Secular geochemistry of central Puerto Rican island arc lavas: Constraints on Mesozoic tectonism in the eastern Greater Antilles: Journal of Petrology, v. 42, p. 2197–2214, https://doi.org/10.1093/petrology/42.12.2197.

Lo, K.Y., and Lee, C.F., 1973, Stress analysis and slope stability in strain-softening materials: Geotechnique, v. 23, p. 1–11, https://doi.org/10.1680/geot.1973.23.1.1.

Lobbestael, A.J., Athanasopoulos-Zekkos, A., and Colley, J., 2013, Factor of safety reduction factors for accounting for progressive failure for earthen levees with underlying thin layers of sensitive soils: Mathematical Problems in Engineering, v. 2013, 893602, p. 1–13, https://doi.org/10.1155/2013/893602.

Locat, J., Leroueil, A., Locat, A., and Lee, H.J., 2014, Weak layers: Their definition and classification from a geotechnical perspective, *in* Krastel, S., et al., eds., Submarine Mass Movements and Their Consequences: Dordrecht, Netherlands, Springer, Advances in Natural Hazard Research, v. 37, p. 3–12, https://doi.org/10.1007/978-3-319-00972-8_1.

Machiels, L., Garces, D., Snellings, R., Vilema, W., Morante, F., Paredes, C., and Elsen, J., 2014, Zeolite occurrence and genesis in the Late-Cretaceous Cayo arc of Coastal Ecuador: Evidence for zeolite formation in cooling marine pyroclastic flow deposits: Applied Clay Science, v. 87, p. 108–119, https://doi.org/10.1016/j.clay.2013.10.018.

Miramontes, E., Cattaneo, A., Jouet, G., Théreau, E., Thomas, Y., Rovere, M., Cauquil, E., and Trincardi, F., 2016, The Pianosa contourite depositional system (northern Tyrrhenian Sea): Drift morphology and Plio-Quaternary stratigraphic evolution: Marine Geology, v. 378, p. 20–42, https://doi.org/10.1016/j.margeo.2015.11.004.

Miramontes, E., Garziglia, S., Sultan, N., Jouet, G., and Cattaneo, A., 2018, Morphological control of slope instability in contourites: A geotechnical approach: Landslides, v. 15, p. 1085–1095, https://doi.org/10.1007/s10346-018-0956-6.

Morgan, J.K., and Clague, D.A., 2003, Volcanic spreading on Mauna Loa volcano, Hawaii: Evidence from accretion, alteration, and exhumation of volcaniclastic sediments: Geology, v. 31, p. 411–414, https://doi.org/10.1130/0091-7613(2003)031<0411:VSOMLV>2.0.CO;2.

Mumpton, F.A., 1999, La roca magica: Uses of natural zeolites in agriculture and industry: Proceedings of the National Academy of Sciences of the United States of America, v. 96, p. 3463–3470, https://doi.org/10.1073/pnas.96.7.3463.

Potts, D.M., Dounias, G.T., and Vaughan, P.R., 1990, Finite-element analysis of progressive failure of Carsington embankment: Geotechnique, v. 40, p. 79–101, https://doi.org/10.1680/geot.1990.40.1.79.

Puzrin, A.M., and Germanovich, L.N., 2005, The growth of shear bands in the catastrophic failure of soils: Proceedings of the Royal Society of Londonz: A, Mathematical, Physical and Engineering Sciences, v. 461, p. 1199–1228.

Puzrin, A.M., Germanovich, L.N., and Friedli, B., 2016, Shear band propagation analysis of submarine slope stability: Geotechnique, v. 66, p. 188–201, https://doi.org/10.1680/jgeot.15.LM.002.

Rohling, E.J., Foster, G.L., Grant, K.M., Marino, G., Roberts, A.P., Tamisiea, M.E., and Williams, F., 2014, Sea-level and deep-sea-temperature variability over the past 5.3 million years: Nature, v. 508, p. 477–482, https://doi.org/10.1038/nature13230.

Venzke, E., ed., 2013, Volcanoes of the World, Volume 4.5.0: Washington, D.C., Smithsonian Institution Global Volcanism Program, https://doi.org/10.5479/si.GVP.VOTW4-2013 (accessed 2 Jul 2016).

Wiemer, G., and Kopf, A., 2015, Altered marine tephra deposits as potential slope failure planes?: Geo-Marine Letters, v. 35, p. 305–314, https://doi.org/10.1007/s00367-015-0408-4.

Zúñiga, D., Garcia-Orellana, J., Calafat, A., Price, N.B., Adatte, T., Sanchez-Vidal, A., Canals, M., Sanchez-Cabeza, J.A., Masque, P., and Fabres, J., 2007, Late Holocene fine-grained sediments of the Balearic Abyssal Plain, Western Mediterranean Sea: Marine Geology, v. 237, p. 25–36, https://doi.org/10.1016/j.margeo.2006.10.034.